

Dynamic entanglement in oscillating molecules and potential biological implicationsJianming Cai,^{1,2} Sandu Popescu,^{3,4} and Hans J. Briegel^{1,2}¹*Institut für Theoretische Physik, Universität Innsbruck, Technikerstraße 25, A-6020 Innsbruck*²*Institut für Quantenoptik und Quanteninformation der Österreichischen Akademie der Wissenschaften, Innsbruck, Austria*³*H.H. Wills Physics Laboratory, University of Bristol, Tyndall Avenue, Bristol BS8 1TL, United Kingdom*⁴*Hewlett-Packard Laboratories, Stoke Gifford, Bristol BS12 6QZ, United Kingdom*

(Received 8 February 2010; revised manuscript received 14 June 2010; published 25 August 2010)

We demonstrate that entanglement can persistently recur in an oscillating two-spin molecule that is coupled to a hot and noisy environment, in which no static entanglement can survive. The system represents a non-equilibrium quantum system which, driven through the oscillatory motion, is prevented from reaching its (separable) thermal equilibrium state. Environmental noise, together with the driven motion, plays a constructive role by periodically resetting the system, even though it will destroy entanglement as usual. As a building block, the present simple mechanism supports the perspective that entanglement can exist also in systems which are exposed to a hot environment and to high levels of decoherence, which we expect, e.g., for biological systems. Our results also suggest that entanglement plays a role in the heat exchange between molecular machines and environment. Experimental simulation of our model with trapped ions is within reach of the current state-of-the-art quantum technologies.

DOI: [10.1103/PhysRevE.82.021921](https://doi.org/10.1103/PhysRevE.82.021921)

PACS number(s): 87.15.-v, 03.65.Ud, 03.65.Yz, 03.67.-a

I. INTRODUCTION

The question, to what extent quantum mechanics plays a role in biology, is still far from being well understood [1,2]. It seems that classical concepts alone are insufficient for a proper understanding of certain biological processes, and that coherent quantum effects need to be taken into account. It has, e.g., long been known that quantum tunneling plays an important role in enzymatic reactions [3,4]. Experimental evidence for quantum coherence in the photosynthetic system and polymers has recently been reported in [5–8]. The interplay between the coherent free Hamiltonian and the environment is believed to significantly enhance quantum transport in the Fenna-Matthews-Olson (FMO) protein complex [9–11]. More generally, one can observe growing interest in the role of quantum coherence and entanglement in specific biological scenarios, e.g., photosynthesis [12–19] and the chemical compass mechanism for magnetoreception [20,21].

Apart from these isolated instances where quantum coherence seems to help, it is however not clear to what extent biological systems exploit quantum mechanics—beyond the trivial fact that the latter determines, of course, the structure of biomolecules—e.g., to optimize their functionality. Most physicists and biologists are generally skeptical about the question whether genuine quantum features such as entanglement play a broader role in biology. The obvious reason for that viewpoint is that entanglement is very sensitive to noise and requires special conditions to be maintained, in particular very good insulation. Biological systems are anything but—they are wet and hot, and with extremely high levels of noise.

An often ignored fact is, however, that biological systems are also open driven quantum systems, operating far away from thermal equilibrium [2]. This opens many new possibilities which have not yet been carefully considered. Different from, e.g., solid state physics, things in biology *move*.

Conformational motion is in fact an omnipresent and important feature of biomolecular processes. Protein function, for example, requires conformational motion [22,23] and so do all kinds of molecular machines. Many of these conformational changes are reversible (under a supply of free energy) and lead to quasiperiodic processes. During such motion, we have to consider time-dependent quantum interactions (capable of forming, e.g., hydrogen or ionic bonds) which are effectively switched on and off while the molecule changes its shape. Since these interactions are accompanied by a substantial amount of noise (e.g., from fluctuating dipole fields from the hydration shell and the bulk solvent), they are usually treated classically. A proper understanding of protein dynamics may however require one to explore the capability of these time-dependent interactions and whether they need to be treated quantum mechanically [24]. It is, for example, not clear whether or not entanglement is generated during these motional processes. A positive answer to this question might reveal novel and subtle aspect of protein dynamics and biomotoric processes. It would also provide a new twist to the study of nanobio interfaces, which are just in their infancy.

In this paper, we investigate the effect of entanglement generation during a nonequilibrium process driven by molecular motion. We introduce a semiclassical picture where the conformational motion of a biomolecule is described classically, but it is assumed that it also carries quantum degrees of freedom, such as nuclear spins and electronic states, which are sufficiently localized on the molecule. Conformational motion then gives rise to effectively time-dependent quantum interactions, with their strengths depending on the molecular shape, see Fig. 1. We analyze the role of environmental noise and decoherence in such interactions. We find that entanglement can be generated even at room temperature and despite the presence of decoherence. This result suggests that the underlying interactions should indeed be treated fully quantum mechanically. It also shows that the usual paradigm, that quantum interactions which are accompanied by signifi-

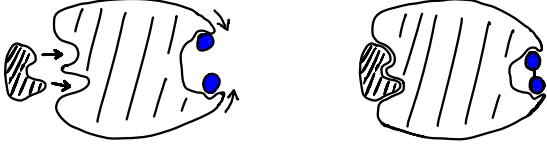


FIG. 1. (Color online) Conformational changes of a biomolecule [23], induced e.g., by the interaction with some other chemical, can lead to a time-dependent interaction between different sites (blue) of the molecule. See also [2].

cant levels of noise (as it is typically the case in a biological environment) may be effectively described by a classical stochastic process, is invalid in our context.

II. SEMIQUANTAL MODEL OF MOLECULAR MOTION

As a paradigmatic example, we study the time-dependent interaction of two spins in a thermal and decoherent environment. We may imagine that the spins are attached to some classical backbone structure whose shape changes in time, as drawn schematically in Fig. 2. For simplicity we call such an arrangement a *two-spin molecule*. We demonstrate that, if the distance between the spins is oscillating, cyclic generation of fresh entanglement can persist, even if no static entanglement can survive. Environmental noise plays thereby both a destructive and constructive role by effectively resetting the system [25]. The oscillating molecule may be viewed as a molecular machine that exchanges heat with the reservoir. Our results then show that, for the chosen interaction, the occurrence of entanglement is always accompanied by the absorption of heat from the environment, which might possibly affect certain biological processes.

In the semiquantal picture that we have introduced, the conformational changes lead to *classical motion of quantum degrees of freedom* as illustrated in Fig. 2. We assume that the two spins are coupled with Ising interaction and that there also exist local electric and/or magnetic fields, both of which are usually position dependent. Thus, the classical molecular motion induces an effective time-dependent Hamiltonian of the form

$$H_M(t) = J(t)\sigma_x^{(1)}\sigma_x^{(2)} + B(t)(\sigma_z^{(1)} + \sigma_z^{(2)}), \quad (1)$$

where $\sigma_x^{(\alpha)}$ and $\sigma_z^{(\alpha)}$ are Pauli operators of the α th spin, $J(t)$ is the interaction strength, and $\omega_0(t) = 2B(t)$ the local level split-

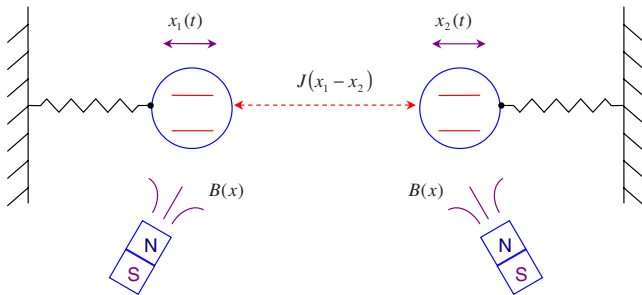


FIG. 2. (Color online) Model of a two-spin molecule which undergoes conformational changes as a function of time. Both the spin-spin interaction strength J and local fields B are position dependent.

ting. We emphasize that the subsequent results also hold for more general Hamiltonians, but for simplicity we concentrate here on the Ising interaction. The coupling of the spins to the environment will be described by a master equation of the form

$$\frac{\partial}{\partial t}\rho(t) = -i[H_M(t), \rho] + \mathcal{D}\rho(t) \equiv \mathcal{L}(t)\rho(t), \quad (2)$$

where $\mathcal{D}\rho = \sum_{\mu} 2L_{\mu}\rho L_{\mu}^{\dagger} - L_{\mu}^{\dagger}L_{\mu}\rho - \rho L_{\mu}^{\dagger}L_{\mu}$ describes the effect of the molecule-environment coupling, and L_{μ} are Lindblad-type generators.

III. PERSISTENT RECURRENCE OF ENTANGLEMENT

The effect of the environment on the motion of biomolecules is complex and far from being understood. To demonstrate the essential physics, we first consider a worst-case scenario, where the environment is described by bosonic heat bath, with each spin being coupled to an independent thermal bath of harmonic oscillators [26,27]. In the static case, it is well known that, above a certain temperature, no initial entanglement can persist in such an environment. We will however show that, even under such unfavorable conditions, entanglement can be generated if the particles start oscillating and the system moves out of equilibrium.

If the molecular oscillation is not too fast, in the sense that the adiabatic condition for closed systems is satisfied, the effect of the environment on the oscillating molecule can be described by a master equation of type (2), with implicitly time-dependent Lindblad generators (see Appendix, Sec.2). As far as the *static entanglement* is concerned, at every molecular configuration (with *fixed* J and B), the molecule will be driven toward its thermal equilibrium state ρ_{th} at temperature T . In the following, we adopt the concurrence $\mathcal{C}(\rho)$ [28] as the measure of two-qubit entanglement of a state ρ . For a separable (nonentangled) state it vanishes, while for a maximal entangled state it reaches the value 1, i.e., $0 \leq \mathcal{C}(\rho) \leq 1$. It can be shown that, if the temperature is above a critical value T_c , no entanglement can survive in any static configuration of the molecule, i.e., $\mathcal{C}(\rho_{th}) = 0$. In the following, we will only consider such situations where $T > T_c$ (see Appendix, Sec.3 and 4 for more details).

The main question we are asking is this: *Can entanglement possibly build up through the classical motion of the molecule?* The answer is affirmative and we demonstrate that entanglement can indeed persistently recur in an oscillating molecule, even if the environment is so hot that the static thermal state is separable for all possible molecular configurations, i.e., $T > \max\{T_c\}$.

Let us first present an intuitive explanation. Consider the following simple process: until time $t=0$, the spins are kept distant (with $J=0$) and the molecule is in the thermal equilibrium state, with the fraction p_g of the population in the ground state ($|\epsilon_0(0)\rangle \approx |\downarrow\downarrow\rangle$). If the local level splitting is sufficiently large such that $\hbar\omega_0(0) \geq k_B T$, p_g will be relatively large compared to the other energy levels. The thermal state will therefore be close to the ground state, which is, in this case, nonentangled. The adiabatic molecular motion from the distant configuration to proximity will transform the

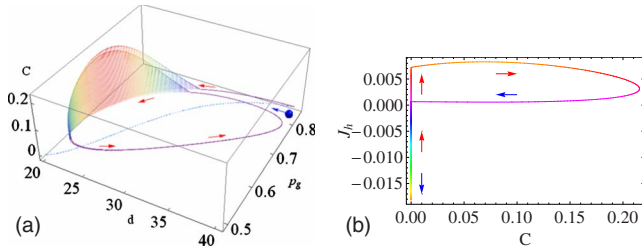


FIG. 3. (Color online) (a) ground-state population p_g and entanglement C vs. the molecular configuration characterized by spin-spin distance d for the bosonic heat bath with unit temperature $T = 1$ and the system-bath coupling strength $\kappa = 0.01$. The blue dashed curve is the instantaneous thermal equilibrium state. The arrows indicate the evolution direction as the molecule oscillates. (b) heat current \mathcal{J}_h vs entanglement C . The oscillation parameters are $x_1(0) = -x_2(0) = -20$, $a = 5$, $\tau = 100$, and $B_0 = 1.3$, $B_1 = 2.4$, $\sigma = 120$, $J_0 = 1 \times 10^4$ [see Eq. (3) and the text thereafter]. We use dimensionless parameters for which the Planck and Boltzmann constants are set to unity, $\hbar = 1$, $k_b = 1$. The temperature $T = 1$ means that we set the thermal energy $k_b T$ as the unit and express the other values as multiples of the thermal energy. For example, $B = 1$ indicates that $\hbar B / k_b T = 1$.

eigenstates of $H_M(0)$ into those of $H_M(t)$; in particular, the ground state $|\epsilon_0(0)\rangle \rightarrow |\epsilon_0(t)\rangle$ will become entangled as the coupling between the spins increases. This explains, qualitatively, why we may expect entanglement to build up in *one run* of a conformational change, given that the molecular motion is slow enough to be adiabatic, but at the same time faster than the thermalization process: Driven through the classical motion, the system is so-to-speak “kicked out” of the (separable) thermal equilibrium state, as can be seen in Fig. 3.

The above analysis only suggests that entanglement may appear during an initial, transient stage of a conformational change. However it does not explain how one can expect to see entanglement on a longer time scale, when the environment begins to mix the internal states as the molecule continues to oscillate. It seems that, in the long run, it may (and will) disappear as usual. What we are interested in, however, is the *persistent* generation of dynamic entanglement, thus a built-in mechanism is necessary to refresh the state of the molecule by resetting it back to the initial state. It is intriguing that this role can be played by environmental noise together with oscillatory motion, both of which naturally exist in biological systems without further need for control.

Let us now present the numerical results which we obtained by numerically integrating Eq. (2). We consider the situation where the spin positions are

$$x_\alpha(t) = x_\alpha(0) + (-1)^\alpha a \left(\cos \frac{2\pi t}{\tau} - 1 \right), \quad (3)$$

where $x_\alpha(0)$ are the initial positions, a is the amplitude of oscillation, and τ is the oscillation period. For the local fields we assume Gaussian functions of the spin position as $B(t) = B_0 - B_1 e^{-x^2(t)/\sigma}$. For the interaction between two spins we assume dipole-dipole coupling $J(t) = J_0 / d^3(t)$ with $d(t) = |x_1(t) - x_2(t)|$. It can be seen from Fig. 3 that recurrent fresh

entanglement appears on the asymptotic cycle. The thermalizing environment is here constructive by repumping the population into the ground state.

For biological systems, $T \approx 300K$, the thermal energy $k_b T$ is about 0,025 eV. Energy scales in biomolecules are typically of the order 0.01–0.5 eV (e.g., for hydrogen bonds or electronic excitation [24,29]) and thus $\hbar \omega_0(0)$ can be several times larger than $k_b T$. The system-bath coupling strength $\kappa = 0.01$ corresponds to a thermalization time of the order of $\sim ps$, which compares e.g., with the time scale of (fast) conformational changes within biomolecules and with relaxation times in the FMO complex [30]. These numbers seem to be consistent with our conclusion that recurrent entanglement might indeed be found in biomolecular processes at room temperature.

The oscillating molecule exhibits rather distinct features of nonequilibrium thermodynamics [31], e.g., the entropy does not always increase with time and reach its saturate value. The most instructive feature is perhaps the connection between entanglement and the heat current \mathcal{J}_h between the molecule and its environment, which is defined by the energy dissipated via the heat bath as [26]

$$\mathcal{J}_h(t) = Tr\{H_M(t)[\mathcal{D}\rho(t)]\}. \quad (4)$$

It can be seen from Fig. 3 that, whenever entanglement appears, $\mathcal{J}_h(t)$ is always positive, i.e., the molecule tends to absorb heat. This can be understood as follows. We first note that no entanglement exists in the thermal equilibrium state, and the corresponding heat current vanishes. When the molecule oscillates, entanglement emerges on the asymptotic cycle mainly because of a relatively larger population of the (entangled) ground state, as compared to the thermal equilibrium state—see Fig. 3(a). The enhanced ground-state population, in turn, leads to a population redistribution from the ground state to the higher-lying energy levels, by which process the molecule tends to absorb heat from its thermal environment. Thus, in the case of our oscillating molecule, the occurrence of entanglement is accompanied with heat absorption. This connection depends of course on the details of the Hamiltonian, e.g., the fact that the ground state is entangled (which is, e.g., the case for the Ising interaction), and as such it cannot be strict and general. However it illustrates an intriguing interplay between entanglement and other thermodynamic quantities for such nonequilibrium systems, which may also be interesting in the context of biomolecular machines. More details, including, e.g., the time dependence of various thermodynamic quantities on the asymptotic cycle, are given in Appendix, Sec.5.

The results discussed so far have been obtained by modeling the noisy environment as an Ohmic bosonic heat bath. Clearly, this is a highly idealized model and in any real biological scenario we have far more complicated interactions, e.g., with the surrounding hydration shell and the bulk solvent [24,32]. We found similar results also with other decoherence models, based on collision-type interactions of the environment with the system [31]. These can be described by Lindblad generators $L_g^{(\alpha)} = \sqrt{\gamma s} \sigma_+^{(\alpha)}$ and $L_d^{(\alpha)} = \sqrt{\gamma(1-s)} \sigma_-^{(\alpha)}$, where γ is the collision-induced effective relaxation rate and s is the mean excitation of a spin in thermal equilibrium. In

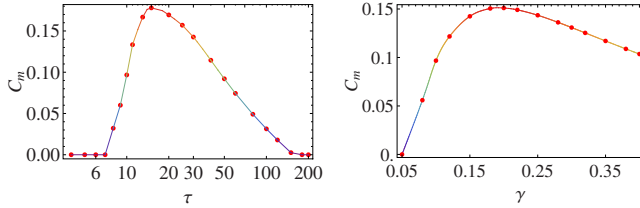


FIG. 4. (Color online) Left: the maximal value of entanglement on the asymptotic cycle C_m vs the oscillation period τ (logarithmic coordinate) with $\gamma=0.1$. Right: C_m vs γ with $\tau=10$. The other parameters are $s=0.2$, $x_1(0)=-x_2(0)=-25$, $a=10$, and $B_0=B_1=1.2$, $\sigma=120$, $J_0=1.2 \times 10^3$.

Fig. 4 we demonstrate the competition between the constructive and destructive effects of environmental noise in such a model, which yields an optimal value for the oscillation period τ to establish entanglement, see Fig. 4(a). For short oscillation periods, efficient thermalization becomes more important: with growing rate γ , the increase in reset efficiency more than compensates the decrease in efficiency of entanglement generation, see Fig. 4(b). In this regime, the net effect of environmental noise is constructive. For more details see Appendix, Sec.6 and 7. The dependence of the entanglement on τ and γ seems reminiscent of what happens in the nice example of quantum “stochastic resonance,” which has been described in a quantum-optical context [33]. That phenomenon is, however, fundamentally different from ours, as it involves a bath at zero temperature, and the noise is the main driving force.

Given the complexity of biological systems, how to characterize biological environment is far from been understood. The effect we presented—i.e., the existence of persistent entanglement—is to a very large extent independent of the precise details of the classical movement, and the thermal bath. Of course, the detailed characteristics of the entanglement (how much entanglement, how does it vary with time, etc.) depend on the driving motion and the specific environment, but the very existence of persistent entanglement is generic (extensible to different types of classical motions, spectral density of thermal bath and also to the non-Markovian environment). A number of different models illustrating this generic property are presented in Appendix, Sec.8.

IV. EXPERIMENTAL SIMULATION

One can test the feasibility of our model by simulating an oscillating molecule in a noisy environment. Two internal levels of trapped ions can encode an effective two-level system. The system Hamiltonian in the form of Eq. (1) is implementable via state-dependent optical dipole forces [34]. The classical oscillation, the essence of which is to introduce a time-dependent Hamiltonian, can be simulated by tuning the interaction strength and the transverse fields, which is achievable, e.g., by changing the amplitudes of laser beams [35–37]. Decoherence can be simulated by, e.g., applying random pulses to induce different decoherence channels. One can also simulate the bosonic bath by engineering the cou-

pling between ions and vacuum modes of the electromagnetic field through laser radiation [38]. Entanglement can finally be detected by performing quantum state tomography as in [39]. Other implementations are conceivable, e.g., using quantum dots mounted on the tips of oscillating cantilevers [40].

ACKNOWLEDGMENTS

We are grateful for the support from the Austrian Science Fund (SFB FoQuS, J.M.C. through Lise Meitner Program) and the European Union (QICS, SCALA, NAMEQUAM). S.P. acknowledges support from the UK EPSRC through the IRC-QIP.

APPENDIX

1. Methods

To account for the effect of the environment on the oscillating two-spin molecule, we have studied different models, two of which we discuss here. In the first model—the bosonic heat bath—each qubit is coupled to an independent thermal bath of harmonic oscillators. This is a well-known decoherence model and the derivation of the master equation (2) follows standard techniques (see e.g., [26]), with the important difference that in our case the Hamiltonian $H_M(t)$ of the system is *time dependent*, i.e., its instantaneous energy spectrum changes as the qubits move. This makes the analysis much more complicated, but under certain conditions it can be still be described by an equation of type (2), albeit with time-dependent Lindblad operators.

In the second model—the spin-gas model [41]—each qubit is subject to random, collision-type interactions with a “background gas” of other spin particles. These processes can lead to both local spin exchange and dephasing. Here we model these processes again by a Lindblad-type master equation [42], but we mention that a numerical treatment including memory effects in the environment, which gives rise to non-Markovian decoherence, can be given [41].

We calculate the entanglement that is generated during the molecular motion, using the two-qubit measure of concurrence [28].

2. Master equation for the oscillating molecule in contact with bosonic heat baths

The derivation of the master equation follows standard arguments used in reservoir theory (see, e.g., [26]), but with some important modifications due to the time dependence of the problem.

One should point out from the outset that the derivation of the master equation rests on a series of assumptions (including e.g., the Born and Markov approximation and the secular or rotating-wave approximation), neither of which we expect to be very well satisfied in real biological systems.

What the master equation *does provide*, however, is a dynamical process that exhibits the essential features that we expect to be most relevant in our system of consideration: a process that is *disentangling* and that leads to decoherence

and thermalization in the subsystem, the two-spin molecule. Whether or not these processes follow, e.g., an exponential decay is not so essential for the main argument.

The total Hamiltonian of the system and the environment can be written in the form

$$H_{tot}(t) = H_M(t) + H_B + H_{MB}, \quad (\text{A1})$$

where $H_M(t)$ is the time-dependent Hamiltonian (1) of the two-spin molecule and H_B , H_{MB} describe the oscillator bath and the molecule-bath interactions, respectively. We assume dissipative coupling, in which case the latter can be written in the form

$$H_{MB} = \sum_{\alpha} \sigma_x^{(\alpha)} \otimes B_{\alpha} \quad (\text{A2})$$

where $B_{\alpha} = B_{\alpha}^{\dagger}$ denote the collective bath degrees of freedom that couple to the α th spin. The interaction constants have been absorbed in the B_{α} s.

Within the usual Born-Markov approximation, one obtains an equation of motion for the two-spin molecule which, in the interaction picture, has the form

$$\frac{\partial}{\partial t} \rho(t) = - \int_0^t ds \text{Tr}_B [H_{MB}(t), [H_{MB}(t-s), \rho(t) \otimes \rho_B]], \quad (\text{A3})$$

where $\rho(t) = \text{Tr}_B \rho_{MB}(t)$ represents the reduced density matrix of the two-qubit molecule after tracing out the degrees of freedom of the thermal baths.

To perform the secular or rotating wave approximation, we expand the spin operators $\sigma_x^{(\alpha)}$ in Eq. (A2) into the basis of instantaneous eigenstates $|\epsilon_i(t)\rangle$ with eigenvalues $\epsilon_i(t)$ ($i = 0, \dots, 3$) of the system Hamiltonian $H_M(t)$, i.e.,

$$\sigma_x^{(\alpha)} = \sum_{\omega(t)} S_{\omega(t)}^{(\alpha)} \quad (\text{A4})$$

$$= \sum_{\omega(t)} \sum_{\epsilon(t) - \epsilon_j(t) = \omega(t)} S_{ij}^{(\alpha)}(t) |\epsilon_i(t)\rangle \langle \epsilon_j(t)|. \quad (\text{A5})$$

In the first line, the operators $S_{\omega(t)}^{(\alpha)}$ describe intramolecular transitions with frequency $\omega(t)$ and the summation runs over all resonant transition frequencies; in the second line, $S_{ij}^{(\alpha)}(t) = \langle \epsilon_i(t) | \sigma_x^{(\alpha)} | \epsilon_j(t) \rangle$ are the corresponding transition matrix elements and the summation runs over all states with matching energy eigenvalues $\epsilon_i(t)$, $\epsilon_j(t)$. In the interaction picture, which is used in the derivation of the master equation, we then write

$$\sigma_x^{(\alpha)}(t) = \sum_{\omega(t)} U^{\dagger}(t) S_{\omega(t)}^{(\alpha)} U(t), \quad (\text{A6})$$

where $U(t)$ is the unitary evolution generated by the system Hamiltonian, $U(t) = \mathcal{T} e^{-i \int_0^t H_M(s) ds}$, and \mathcal{T} denotes the time ordering operator.

In a situation where the system's evolution is *adiabatic*, i.e., slow enough to avoid energy-changing transitions, the eigenstates will only pick up a dynamic phase (under the coherent evolution of the time-dependent system Hamiltonian) [31]. The time dependence of the spin operators in

the interaction picture then acquires the simple form

$$\sigma_x^{(\alpha)}(t) = \sum_{\omega(\cdot)} e^{-i \int_0^t \omega(s) ds} \sum_{\epsilon_i(t) - \epsilon_j(t) = \omega(t)} S_{ij}^{(\alpha)}(t) |\epsilon_i(0)\rangle \langle \epsilon_j(0)|. \quad (\text{A7})$$

Upon inserting this into Eq. (A3) and applying (a generalization of) the secular approximation [26], we obtain a master equation of the form (2) with implicitly time-dependent Lindblad operators [31]. The properties of the baths thereby enter through the following Fourier-type transform of the bath correlation functions

$$\Gamma_{\alpha\beta}[\omega(\cdot), t] = \int_0^{\infty} ds e^{i \int_{t-s}^t \omega(s) ds} \langle B_{\alpha}^{\dagger}(s) B_{\beta}(0) \rangle, \quad (\text{A8})$$

which is different from the exact Fourier transform obtained in case of a time-independent system Hamiltonian. For independent baths, we only get a contribution for $\alpha = \beta$. The Markov approximation assumes that the correlation functions $\langle B_{\alpha}^{\dagger}(s) B_{\alpha}(0) \rangle$ decay fast compared to the relaxation time, which means that their real and imaginary part can essentially be replaced by the delta function $\delta(t)$ and its time derivative $\delta'(t)$, respectively. It is therefore consistent to apply, for small values of s , the following approximation for the integral in Eq. (A8),

$$\int_{t-s}^t \omega(t') dt' \approx \omega(t)s. \quad (\text{A9})$$

In summary, we can thus write

$$\Gamma_{\alpha\beta}[\omega(\cdot), t] \approx \delta_{\alpha\beta} \Gamma_{\omega(t)}, \quad (\text{A10})$$

where the function $\Gamma_{\omega(t)}$ now depends only on the value of the frequency $\omega(t)$ at the time t . Upon transforming back to the Schrödinger picture, $|\epsilon_i(0)\rangle$ in the transition operators $\sigma_x^{(\alpha)}(t)$ are mapped to $|\epsilon_i(t)\rangle$, and we finally obtain a master equation with the implicitly time-dependent Lindblad generators

$$L_{\mu} \equiv L_{\alpha}(\omega(t)) = \Gamma_{\omega(t)}^{1/2} \sum_{\Delta_{ij}(t) = \omega(t)} S_{ij}^{(\alpha)}(t) |\epsilon_i(t)\rangle \langle \epsilon_j(t)|. \quad (\text{A11})$$

The index $\mu \equiv \{\alpha, \omega(t)\}$ in Eq. (2) runs here over $\alpha = 1, 2$ and over the allowed values of $\omega(t)$. The relevant quantity of the heat bath which enters $\Gamma_{\omega(t)}$ is its spectral density function. If we assume an Ohmic spectral density with infinite cut-off frequency, we obtain

$$\Gamma_{\omega(t)} = \kappa \omega(t) (1 + N_{\omega(t), \beta}), \quad (\text{A12})$$

where $N_{\omega(t), \beta}$ is the bosonic distribution function at inverse temperature β , i.e., $N_{\omega(t), \beta} = 1 / (e^{\omega(t)\beta} - 1)$. The master equation (2) with these Lindblad operators was used to calculate the data shown in Fig. 3.

3. Concurrence and static thermal entanglement

To measure the dynamic entanglement generated during molecular oscillation, we compare it with the thermal equi-

librium state when the molecular configuration is fixed at any distance. In such a “static configuration,” both the Hamiltonian and the Lindblad operators are time independent. Furthermore, the derived quantum master equation is then *mixing* and the molecule will always be driven to its thermal equilibrium state [26] corresponding to the reservoir temperature $\beta=1/T$. For each specific molecular configuration, with fixed spin-spin interaction strength J and local electric or magnetic fields B , the thermal equilibrium state reads

$$\rho_{th} = e^{-\beta H_M} / \mathcal{Z} = \frac{1}{\mathcal{Z}} \begin{pmatrix} r_{00} & 0 & 0 & r_{03} \\ 0 & r_{11} & r_{12} & 0 \\ 0 & r_{21} & r_{22} & 0 \\ r_{30} & 0 & 0 & r_{33} \end{pmatrix}, \quad (\text{A13})$$

where $\mathcal{Z} = \text{Tr}(e^{-\beta H_M})$ is the partition function and the matrix representation refers to the computational product basis. The nonzero entries of the above matrix are given by

$$r_{00} = e^{\mathcal{E}\beta} - 2 \sinh(\mathcal{E}\beta) / (1 + \eta^2), \quad (\text{A14})$$

$$r_{11} = r_{22} = \cosh(J\beta), \quad (\text{A15})$$

$$r_{33} = e^{-\mathcal{E}\beta} + 2 \sinh(\mathcal{E}\beta) / (1 + \eta^2), \quad (\text{A16})$$

$$r_{03} = -J \sinh(\mathcal{E}\beta) / \mathcal{E}, \quad r_{12} = -\sinh(J\beta) \quad (\text{A17})$$

where $\mathcal{Z} = 2[\cosh(\mathcal{E}\beta) + \cosh(J\beta)]$, $\mathcal{E} = (4B^2 + J^2)^{1/2}$, and $\eta = (\mathcal{E} - 2B)/J$. To quantify the two-qubit entanglement, there exist various kinds of entanglement measures. We choose the concurrence C [28], which is defined as $C = \max\{0, \lambda_1 - \lambda_2 - \lambda_3 - \lambda_4\}$, where the λ_i s are the square roots of the eigenvalues of $\rho \tilde{\rho}$ in decreasing order [28], with $\tilde{\rho} = (\sigma_y \otimes \sigma_y) \rho^* (\sigma_y \otimes \sigma_y)$. For the thermal equilibrium state (A13), one obtains

$$C(\rho_{th}) = \frac{2}{\mathcal{Z}} \max\{0, |r_{12}| - (r_{00}r_{33})^{1/2}, |r_{03}| - (r_{11}r_{22})^{1/2}\}. \quad (\text{A18})$$

Using the explicit expressions for r_{12}, r_{00}, r_{33} one finds that $|r_{12}| - (r_{00}r_{33})^{1/2} \leq 0$ and $|r_{03}| - (r_{11}r_{22})^{1/2} = \frac{|J|}{\mathcal{E}} \sinh(\mathcal{E}\beta) - \cosh(J\beta)$.

The static thermal entanglement can thus be written as

$$C(\rho_{th}) = \frac{2}{\mathcal{Z}} \max\left\{0, \frac{|J|}{\mathcal{E}} \sinh(\mathcal{E}\beta) - \cosh(J\beta)\right\}. \quad (\text{A19})$$

In order to illustrate how the static entanglement changes as the temperature increases, we calculate the first derivative of C with respect to β . After some straightforward calculations, it can be seen that

$$\partial C(\rho_{th}) / \partial \beta \geq 0, \quad (\text{A20})$$

which means that the static entanglement always decreases as the temperature increases. This is consistent with our intuition that there exists a critical temperature T_c , above which no static entanglement can survive. In other words, for any fixed molecular configuration, entanglement will eventually vanish when the reservoir is too hot. In the main text, we consider exactly such a situation. The temperature of the

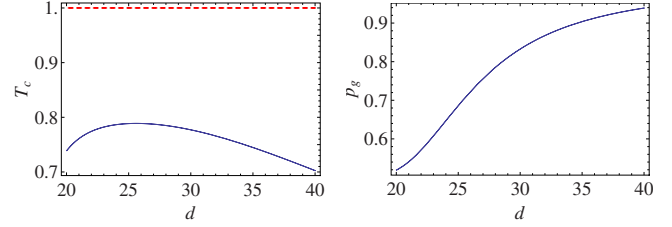


FIG. 5. (Color online) Left: the critical temperature T_c above which any static entanglement disappears vs the molecular configuration d , see the solid curve. For comparison, the red dashed line gives the temperature used in our simulation, which is much higher than the critical temperature at all possible molecular configurations. Right: the ground-state population p_g corresponding to the thermal equilibrium state at the critical temperature T_c .

environment is so high that the thermal state is separable (nonentangled) at all possible molecular configurations, i.e., $T > \max\{T_c\}$.

4. Critical temperature for static entanglement

In Fig. 5, we plot the critical temperature T_c as a function of the distance d between the spins. T_c is defined as the temperature above which entanglement disappears in the thermal equilibrium state of a given static configuration. The temperature chosen in our simulations (e.g., Fig. 3, left), which is chosen as unit in Fig. 5, is indeed much higher for all values of d .

This means that, through the classical motion, dynamic entanglement is recurrently generated at a temperature where no static entanglement can survive. For comparison, we also plot the corresponding ground-state population p_g at the critical temperature. As expected, p_g is close to unity at the distant configuration, since there the ground state is only slightly entangled. The general dependance of the critical temperature on the distance d is less straightforward, as it depends not only on the ground-state entanglement but also on the energy gap.

5. Thermodynamic properties of the oscillating molecule

Here, we present more details about the evolution of some thermodynamic quantities as the molecule undergoes conformational oscillations. To begin with, it is clear that thermodynamic quantities are, in general, well defined only at equilibrium and in the thermodynamic limit. However under certain conditions it can be instructive to extend these definitions to molecular systems and to nonequilibrium situations. In order to justify these extensions in the present case, we first take a look at the form of the molecular state during the asymptotic cycle. If the adiabatic condition for closed quantum systems is satisfied, the molecule that is initially in the eigenstate of the Hamiltonian $H_M(0)$ will remain in the corresponding eigenstate of the Hamiltonian $H_M(t)$ at a later time t . This implies that, on the asymptotic cycle, the density matrix of the system will, at every time t , be diagonal in the instantaneous eigenbasis of $H_M(t)$. This can be verified quantitatively by calculating the fidelity between $\rho(t)$ and the corresponding diagonal state $\rho_0(t) = \sum_i p_i(t) |\epsilon_i(t)\rangle \langle \epsilon_i(t)|$, where

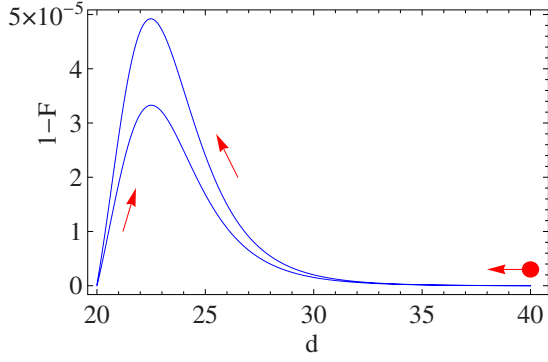


FIG. 6. (Color online) Deviation of the system density matrix $\rho(t)$ from the corresponding diagonal density matrix $\rho_0(t)$, quantified by $1-F$, vs the molecular configuration d on the asymptotic cycle. The red dot and arrow indicate the starting point and the direction of evolution, respectively. The oscillation parameters are the same as in Fig. 3.

$p_i(t) = \langle \epsilon_i(t) | \rho(t) | \epsilon_i(t) \rangle$ is the population of the i th eigenstate of $H_M(t)$, and

$$F(\rho(t), \rho_0(t)) = \text{tr} \sqrt{\rho_0^{1/2}(t) \rho(t) \rho_0^{1/2}(t)} \quad (\text{A21})$$

is the fidelity. It can be seen from Fig. 6 that $F \geq 1 - 10^{-4}$ for the oscillating molecule with the same parameters as in Fig. 3. We may thus tentatively adopt the usual definitions for the entropy and mean energy, based on the probability distribution $p_i(t)$.

We first consider the entropy $\mathcal{S}(t)$ and the internal energy $\mathcal{U}(t)$ defined as follows

$$\mathcal{S}(t) = - \sum_i p_i(t) \ln p_i(t) \quad (\text{A22})$$

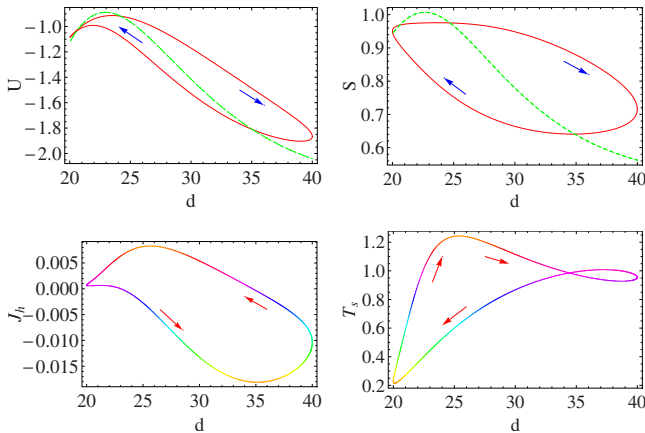


FIG. 7. (Color online) Internal energy \mathcal{U} , entropy \mathcal{S} , heat current \mathcal{J}_h and spectral temperature T_s vs the molecular configuration d on the asymptotic cycle. The oscillation parameters are the same as in Fig. 3. The green dashed curves represent the thermal equilibrium state at each molecular configuration. The blue and red arrows indicate the evolution direction.

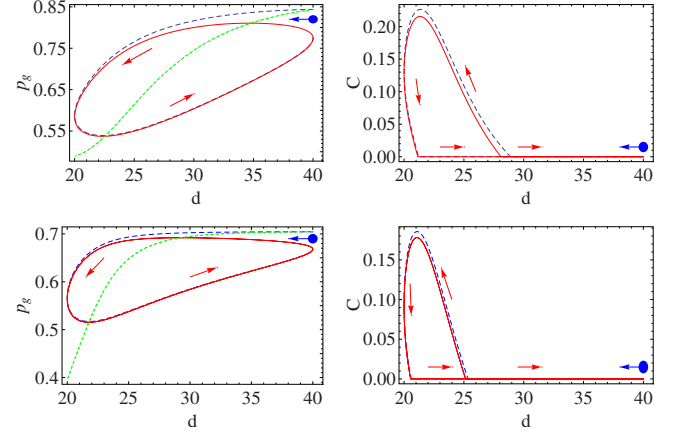


FIG. 8. (Color online) Ground-state population p_g (left) and dynamic entanglement C (right) vs. the molecular configuration d . Upper: Bosonic thermal bath at temperature $T=1$ and $\kappa=0.01$; Lower: spin gas model with $s=0.16$ and $\gamma=0.025$. The oscillation parameters are the same as in Fig. 3. The first cycle and the asymptotic cycle are indicated by the blue dashed and red solid curves, respectively. The green dotted curves (left) represent the instantaneous steady state corresponding to each molecular configuration. The blue dot and arrows indicate the starting point and the evolution direction.

$$\mathcal{U}(t) = \sum_i \epsilon_i(t) p_i(t). \quad (\text{A23})$$

In the static case, i.e., for any fixed configuration ($d=\text{const.}$), thermalization always increases the entropy which approaches its maximum value in the long-time limit. Similarly, the internal energy will approach its static equilibrium value. In the dynamic case, i.e., for the oscillatory motion [Eq. (3)], the situation is quite different and the system will never reach its thermal equilibrium state, as can be seen already in Figs. 8 and 9 shown above. In Fig. 7 we show the evolution of $\mathcal{S}(t)$ and $\mathcal{U}(t)$ on the asymptotic cycle. One can see that their dynamic behavior changes dramatically as the molecule oscillates. First of all, the entropy no longer increases monotonically. Roughly speaking, it increases when two spins come close, but decreases when they move apart.

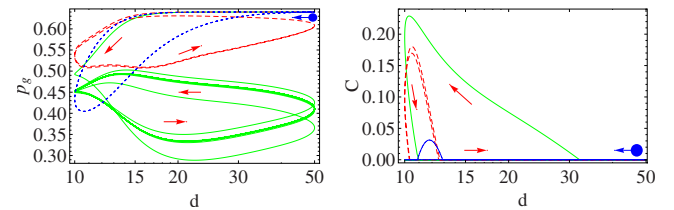


FIG. 9. (Color online) Ground-state population p_g (left) and dynamic entanglement C (right) vs the molecular configuration d (logarithmic coordinate). The oscillation periods are $\tau=6$ (green, solid, gray), 20 (red, dashed, dark gray) and 100 (blue, dotted, light gray) respectively. The dot and arrow indicate the starting point and the evolution direction. Right: the green solid curve (with positive values) only represents the first cycle, while subsequent cycles collapse onto the abscissa, without entanglement. The other parameters are the same as in Fig. 4 (left).

A similar observation can be made for the internal energy. (In the region when the spin become very close this rough description must be refined. There, the details of the rate of change of the energy spectrum, as compared to the thermalization rate, become important). The increase of entropy has to do with the fact that the energy gap between ground and the first excited state decreases as the spins come close and vice versa. The decrease of entropy in the remote configuration effectively resets the molecule into a fresh state of low entropy (i.e., larger purity), after which it is ready to become re-entangled in the subsequent oscillation. This supports our claim about the constructive role of thermalization in the above section.

As we have discussed in the main text, a heat current $\mathcal{J}(t)$ between the molecule and the thermal bath can be defined by the rate of change of the internal energy due to the (dissipative) interaction with the thermal bath as [26]

$$\mathcal{J}(t) = \text{Tr}\{H_m(t)[\mathcal{D}\rho(t)]\}. \quad (\text{A24})$$

Based on this definition, the total heat exchange during a time interval $[t_1, t_2]$ is given by

$$\Delta Q = \int_{t_1}^{t_2} \mathcal{J}_h(t) dt. \quad (\text{A25})$$

If the molecule stays in the thermal equilibrium state (static scenario), the heat current will be zero $\mathcal{J}_h^{(s)}(t)=0$, and thus no heat will be exchanged. For the oscillating molecule, in contrast, the heat current $\mathcal{J}_h(t)$ can be either positive or negative, as is shown in Fig. 7 on the asymptotic cycle. In comparing Fig. 7 with Fig. 3(a), we see that whenever the two spins are entangled, the heat current $\mathcal{J}_h(t)$ is positive, i.e., the molecule absorbs heat from the thermal reservoir. Note that this is a specific property of Hamiltonian Eq. (1), as discussed in the main text.

Since the molecule is not in thermal equilibrium one cannot adopt the standard definition of temperature. Nevertheless, its state is diagonal in the instantaneous eigenbasis of $H_M(t)$. In this case, one can define the so-called inverse spectral temperature as in [43,44],

$$\frac{1}{T_s} = \left(1 - \frac{p_0 + p_3}{2}\right)^{-1} \sum_{i=1}^3 \frac{p_i + p_{i-1}}{2} \beta_{i,i-1} \quad (\text{A26})$$

where $\beta_{i,i-1} = -(\ln p_i - \ln p_{i-1}) / \Delta_{i,i-1}$ corresponds to the ‘‘temperature’’ associated with two neighboring energy levels (viewed as a fictitious two-level system coupled to a heat bath) with energy gap $\Delta_{i,i-1} = \epsilon_i - \epsilon_{i-1}$. If the system is in thermal equilibrium, the spectral temperature reduces to the standard temperature. Based on the definition of spectral temperature, one would say (see Fig. 7) that the molecule is cooled down (or heated up) through its classical motion, whereas the attached thermal bath is always at a fixed higher temperature. While the interpretation of the spectral temperature needs to be taken with caution on general grounds, its characteristics in Fig. 7 is consistent with the observed heat exchange with the environment.

6. Spin-gas model for the environment

The environment of biomolecular systems is rather complex [45] and not yet fully understood, and some of its features may not be well-described by a thermal bath model of harmonic oscillators. To check whether the observed effects are robust, we have also considered an alternative model—the so-called spin gas model [41,42]—for the environment. In this model, we assume collisions between the molecular spins and other, randomly moving spin-particles that constitute the environment. The collisions induce local energy dissipation (i.e., spin exchange) and de-phasing, which leads to decoherence and, if left alone, quickly destroys all entanglement between the molecular spins [46].

The spin-gas model of the environment has been described in Refs. [41,42]. For Ising-type interactions, one can calculate the time evolution of small subsystems exactly, for environments consisting of up to 10^5 – 10^6 particles, without any approximations. Under certain conditions, one can again derive a master equation by considering the effect of random collisions on a coarse-grained time scale [42]. For the present purpose, we will employ such a phenomenological description, but we emphasize that non-Markovian and collective effects in the environment can be taken into account [41].

The effect of random collisions leads to Lindblad generators of the form $L_i \in \{L_g^{(\alpha)}, L_d^{(\alpha)} | \alpha=1, 2\}$ with

$$L_g^{(\alpha)} = \sqrt{\gamma s} \sigma_+^{(\alpha)} \quad \text{and} \quad L_d^{(\alpha)} = \sqrt{\gamma(1-s)} \sigma_-^{(\alpha)}, \quad (\text{A27})$$

where $\sigma_{\pm}^{(\alpha)} = (\sigma_x^{(\alpha)} \pm i\sigma_y^{(\alpha)})/2$ are the Pauli ladder operators for a two-level system. The resulting master equation [42], describes local energy gain and loss processes (‘‘spin exchange’’) with the effective rate $\gamma > 0$, while s is related to the temperature and determines the equilibrium distribution of the local excitation [42]. Without loss of generality, we may assume that the $\gamma > 0$ and $0 \leq s \leq 1/2$. If s is larger than a critical value s_c , no static entanglement can exist [31], similar as in the case of the bosonic heat bath in the previous section.

Even though this model is quite different from the bosonic heat bath, it has certain features in common, for example, it is disentangling and mixing. Remarkably, we find the same phenomenon as in case of the bosonic heat bath, namely, a persistent recurrence of fresh entanglement in a regime where the static entanglement vanishes for all molecular configurations.

In Fig. 8 we compare the evolution of the oscillating molecule for the spin gas model and the bosonic heat bath model. The upper panel of Fig. 8 reproduces the left three-dimensional (3D) plot in Fig. 3 (left) by projecting it onto two dimensional curves. The lower panel shows the same evolution for the spin gas model. It can be seen that the *qualitative* features are robust: During the first oscillation, entanglement builds up when the spins approach each other, while the evolution subsequently converges toward an asymptotic cycle on which the entanglement periodically recurs. This observation strengthens our claim that this feature is robust and does not seem to depend on the detailed features of the environment.

7. Competing effects of environmental noise on dynamic entanglement

Another benefit of the phenomenological spin-gas model is that it allows one to enter the regime of short oscillation periods and to clearly illustrate the competition between the constructive and the destructive effects of the environmental noise [47]. In Fig. 4, we have plotted the maximal value of entanglement that is assumed on the asymptotic cycle, in the case where $s=0.2 > s_c$ (i.e., the equilibrium state is separable for all possible molecular configurations). The left plot displays the maximally achievable entanglement for different oscillation periods. It can be seen that the occurrence of dynamic entanglement strongly depends on the oscillation period; there are competing effects of the environmental noise which give rise to an optimal oscillation period where the effect is most pronounced.

To understand the results in Figs. 4 and 9 better, it is worth looking at the detailed time evolution of the entanglement and the ground-state population for three typical oscillation periods.

First, consider a very long oscillation period, e.g., $\tau = 100$. Here, the molecule is almost completely reset by thermalization to equilibrium when the spins are spatially separated (distant configuration), with a large ground-state population of up to $\sim 65\%$, see Fig. 9 (blue curve). Since in this regime the coherent evolution of the molecule is adiabatic, the population of the instantaneous eigenstates of the system Hamiltonian remains approximately constant, while the off-diagonal elements remain negligible. When two spins come closer, they start interacting and the ground state becomes entangled (entanglement generation regime). If there were no dissipation, the high population of the ground state alone would be sufficient to generate entanglement. However, while the spins approach each other, the energy separation between the lowest lying levels decreases and the dissipation starts repopulating the levels. This drives the molecular state into the separable regime and diminishes its entanglement, with only little entanglement surviving. For a moderate oscillation period, e.g., $\tau=20$ (red curve), the dissipation still has enough time to reset the system while it passes through the distant configuration, with a ground-state population similar as for as $\tau=100$. In the entanglement generation regime, however, the destructive effect of the dissipation is now much smaller than for long oscillation period, which leads overall to more entanglement. Finally, for a very short oscillation period, e.g., $\tau=6$, the destructive effect during the entanglement generation regime is even smaller. On the other hand, the reset effect in the distant configuration is greatly suppressed, since the system does not have enough time to thermalize and to repopulate the ground state. Thus, even though the transient entanglement is larger in the first period, as expected, it will diminish in subsequent runs and cannot be sustained on the asymptotic cycle, due to the lack of an effective reset mechanism.

8. Generic features of persistent dynamic entanglement in noisy environment

In the main text, we have used a simple model, namely a harmonically oscillating molecule in an Ohmic thermal bath,

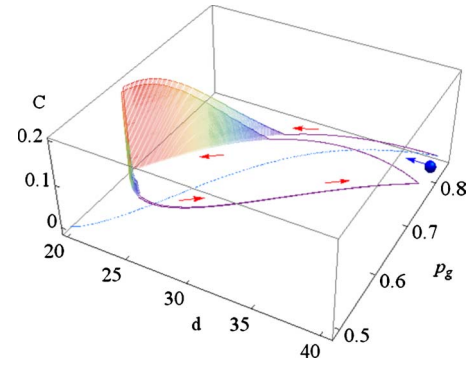


FIG. 10. (Color online) Ground-state population p_g and entanglement C vs the molecular configuration characterized by spin-spin distance d for the bosonic heat bath. The spins move toward (away) from each other with a constant speed. The other parameters are the same as Fig. 3.

to demonstrate the essential mechanism for persistent dynamical entanglement to occur in a de-coherent environment where no static entanglement can exist. Here we show that neither the harmonic oscillatory motion nor the Ohmic thermal bath are indispensable for such an effect. The existence of persistent dynamic entanglement is to a very large extent independent of the precise details of the classical motion and thermal environment.

In Fig. 10, we consider a model where the spins move toward (away) from each other with a constant speed, and observe similar results as for the harmonic oscillatory motion. The same effect can also be seen in a scenario of stochastic movements [31]. In short, the detailed characteristics of the entanglement (how much entanglement, how does it vary with time, etc.) depend on the driving oscillation, but the very existence of persistent entanglement is generic. All that is needed is that the classical motion obeys two conditions: (i) is adiabatically slow but sufficiently fast compared to decoherence and (ii) it spends long enough time at the far end for thermalization to occur.

Regards the model for the bath, we have so-far used the Ohmic bath (as well as the spin-gas model) as an example. However, our results are also valid for other forms of spectral densities. It can be seen from Fig. 11 that the effect of persistent dynamic entanglement is not restricted to the simple Ohmic bath, but occurs also for the sub-Ohmic and supra-Ohmic bath, i.e., for a spectral density $\sim \omega^s$ with s

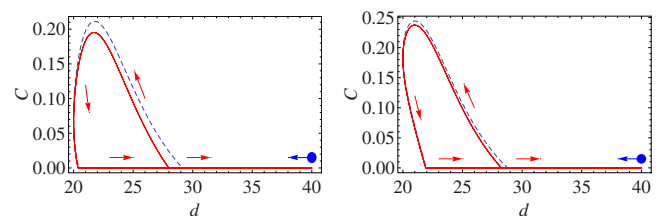


FIG. 11. (Color online) Dynamic entanglement C vs the molecular configuration d for the sub-Ohmic (left, $s=0.8$) and supra-Ohmic (right, $s=1.2$) thermal bath. The other parameters are the same as Fig. 3. The blue dot and red arrows indicate the starting point and the evolution direction. The first cycle and the asymptotic cycle are indicated by the blue dashed and red solid curves, respectively.

<1 or $s > 1$. We have also found that the present mechanism works even with the spectral density from the solvent and protein environment [24], e.g., a spectral density in the form of $\sim \frac{1}{\omega}$. Finally, by using the numerical method of quasiadia-

batic propagator path integral [48,49], we have extended the results to the non-Markovian environment with finite memory time, and still see the generic effect discussed in the main text. More details will be presented in [31].

-
- [1] *Quantum Aspects of Life*, edited by D. Abbott, P. C. W. Davies, and A. K. Pati (World Scientific, Singapore, 2008).
- [2] H. J. Briegel and S. Popescu, e-print [arXiv:0806.4552](https://arxiv.org/abs/0806.4552).
- [3] P. Ball, *Nature (London)* **431**, 396 (2004).
- [4] P. L. Dutton *et al.*, *Philos. Trans. R. Soc. London, Ser. B* **361**, 1293 (2006).
- [5] G. S. Engel *et al.*, *Nature (London)* **446**, 782 (2007).
- [6] H. Lee *et al.*, *Science* **316**, 1462 (2007).
- [7] E. Collini and G. D. Scholes, *Science* **323**, 369 (2009).
- [8] G. Panitchayangkoon *et al.*, e-print [arXiv:1001.5108](https://arxiv.org/abs/1001.5108).
- [9] M. Mohseni *et al.*, *J. Chem. Phys.* **129**, 174106 (2008).
- [10] P. Rebentrost *et al.*, *New J. Phys.* **11**, 033003 (2009).
- [11] M. B. Plenio and S. F. Huelga, *New J. Phys.* **10**, 113019 (2008).
- [12] M. Sarovar, A. Ishizaki, G. R. Fleming, and K. B. Whaley, *Nat. Phys.* **6**, 462 (2010).
- [13] F. L. Semião, K. Furuya, and G. J. Milburn, e-print [arXiv:0909.1846](https://arxiv.org/abs/0909.1846).
- [14] T. Scholak *et al.*, e-print [arXiv:0912.3560](https://arxiv.org/abs/0912.3560).
- [15] A. W. Chin, A. Datta, F. Caruso, S. Huelga, and M. Plenio, *New J. Phys.* **12**, 065002 (2010).
- [16] M. M. Wilde, J. M. McCracken, and A. Mizel, *Proc. R. Soc. London, Ser. A* **466**, 1347 (2010).
- [17] F. Caruso, A. Chin, A. Datta, S. Huelga, and M. Plenio, *Phys. Rev. A* **81**, 062346 (2010).
- [18] K. Bradler, M. M. Wilde, S. Vinjanampathy, and D. B. Uskov, e-print [arXiv:0912.5112](https://arxiv.org/abs/0912.5112).
- [19] X.-T. Liang, e-print [arXiv:1001.0809](https://arxiv.org/abs/1001.0809).
- [20] J. Cai, G. G. Guerreschi, and H. J. Briegel, *Phys. Rev. Lett.* **104**, 220502 (2010).
- [21] E. Gauger, E. Rieper, J. J. L. Morton, S. C. Benjamin, and V. Vedral, e-print [arXiv:0906.3725](https://arxiv.org/abs/0906.3725).
- [22] H. Frauenfelder, P. G. Wolynes, and R. H. Austin, *Rev. Mod. Phys.* **71**, S419 (1999).
- [23] B. Alberts *et al.*, *Molecular Biology of the Cell* (Garland Science, New York, 2008).
- [24] J. Gilmore and R. H. McKenzie, *J. Phys. Chem. A* **112**, 2162 (2008).
- [25] L. Hartmann, W. Dür, and H. J. Briegel, *Phys. Rev. A* **74**, 052304 (2006).
- [26] H. P. Breuer and F. Petruccione, *The Theory of Open Quantum Systems* (Oxford University Press, New York, 2002).
- [27] J. Gilmore and R. H. McKenzie, *J. Phys.: Condens. Matter* **17**, 1735 (2005).
- [28] W. K. Wootters, *Phys. Rev. Lett.* **80**, 2245 (1998).
- [29] A. Olaya-Castro, C. F. Lee, F. F. Olsen, and N. F. Johnson, *Phys. Rev. B* **78**, 085115 (2008).
- [30] J. Adolphs and T. Renger, *Biophys. J.* **91**, 2778 (2006).
- [31] J.-M. Cai, G. G. Guerrechi, S. Popescu, H. J. Briegel, (unpublished).
- [32] P. W. Fenimore *et al.*, *Proc. Natl. Acad. Sci. U.S.A.* **101**, 14408 (2004).
- [33] M. B. Plenio and S. F. Huelga, *Phys. Rev. Lett.* **88**, 197901 (2002).
- [34] D. Porras and J. I. Cirac, *Phys. Rev. Lett.* **92**, 207901 (2004).
- [35] A. Friedenauer *et al.*, *Nat. Phys.* **4**, 757 (2008).
- [36] C. Ospelkaus, C. E. Langer, J. M. Amini, K. R. Brown, D. Leibfried, and D. J. Wineland, *Phys. Rev. Lett.* **101**, 090502 (2008).
- [37] Ch. Wunderlich, *In Laser Physics at the Limit* (Springer, New York, 2001), p. 261.
- [38] J. F. Poyatos, J. I. Cirac, and P. Zoller, *Phys. Rev. Lett.* **77**, 4728 (1996).
- [39] C. F. Roos, G. P. T. Lancaster, M. Riebe, H. Haffner, W. Hansel, S. Gulde, C. Becher, J. Eschner, F. Schmidt-Kaler, and R. Blatt, *Phys. Rev. Lett.* **92**, 220402 (2004).
- [40] D. Bouwmeester, private communication.
- [41] L. Hartmann, J. Calsamiglia, W. Dur, and H. J. Briegel, *Phys. Rev. A* **72**, 052107 (2005).
- [42] L. Hartmann, W. Dür, and H. J. Briegel, *New J. Phys.* **9**, 230 (2007).
- [43] G. Mahler, J. Gemmer, and M. Michel, *Physica E* **29**, 53 (2005).
- [44] J. Gemmer, M. Michel, and G. Mahler, *Quantum Thermodynamics* (Springer Press, New York, 2004).
- [45] H. Frauenfelder *et al.*, *Proc. Natl. Acad. Sci. U.S.A.* **106**, 5129 (2009).
- [46] The spin-gas model should not be confused with the spin-bath model [50], which is similar but assumes a static distribution of random couplings between the molecular and the environmental spins.
- [47] We remark that the task of deriving a simple master equation that is also valid for fast oscillations (i.e. beyond the adiabatic approximation) becomes very hard in the case of the bosonic thermal bath.
- [48] N. Makri and D. E. Makarov, *J. Chem. Phys.* **102**, 4600 (1995).
- [49] N. Makri and D. E. Makarov, *J. Chem. Phys.* **102**, 4611 (1995).
- [50] N. V. Prokof'ev and P. C. E. Stamp, *Rep. Prog. Phys.* **63**, 669 (2000).